



Cite this: *Analyst*, 2023, **148**, 3971

## Molecular imprinting-based ratiometric fluorescence sensors for environmental and food analysis

Yuhao Wen,<sup>a,b</sup> Dani Sun,<sup>b,c</sup> Yue Zhang,<sup>b</sup> Zhong Zhang,<sup>d</sup> Lingxin Chen<sup>b,e</sup> and Jinhua Li<sup>\*a,b,c</sup>

Environmental protection and food safety are closely related to the healthy development of human society; there is an urgent need for relevant analytical methods to determine environmental pollutants and harmful substances in food. Molecular imprinting-based ratiometric fluorescence (MI-RFL) sensors, constructed by combining molecular imprinting recognition and ratiometric fluorescence detection, possess remarkable advantages such as high selectivity, anti-interference ability, high sensitivity, non-destruction and convenience, and have attracted increasing interest in the field of analytical determination. Herein, recent advances in MI-RFL sensors for environmental and food analysis are reviewed, aiming at new construction strategies and representative determination applications. Firstly, fluorescence sources and possible sensing principles are briefly outlined. Secondly, new imprinting techniques and dual/ternary-emission fluorescence types that improve sensing performances are highlighted. Thirdly, typical analytical applications of MI-RFL sensors in environmental and food samples are summarized. Lastly, the challenges and perspectives of the MI-RFL sensors are proposed, focusing on improving sensitivity/visualization and extending applications.

Received 29th March 2023,  
Accepted 14th July 2023

DOI: 10.1039/d3an00483j

rsc.li/analyst

### 1. Introduction

At present, environmental pollution and food safety are causing widespread concerns, as the saying goes, “Protecting the environment is everyone’s responsibility” and “Foodstuff is all-important to the people”. Economically thriving societies are not supposed to come up at the expense of the environment. What’s more, as people’s quality of life gets better and better, food safety is becoming more and more significant. Food safety means that food is non-toxic, harmless, meets the expected nutritional requirements, and does not cause any acute, subacute or chronic harm to human health.<sup>1</sup> Related

analytical technologies and methods are imperative for environmental monitoring and food safety.

Environmental and food analysis faces challenges such as complex sample composition, serious matrix interference, low content of components and poor stability.<sup>1,2</sup> Nowadays, the analytical methods used for environmental and food analysis mainly include high performance liquid chromatography (HPLC), capillary electrophoresis (CE), HPLC-mass spectrometry (HPLC-MS), gas chromatography-MS (GC-MS) and biological methods.<sup>3</sup> However, these analytical methods are often suitable only for laboratory research and are difficult for outdoor field experiments. Chromatography is a kind of commonly used qualitative and quantitative detection technique;<sup>3</sup> HPLC-MS has the advantages of high sensitivity, low limit of detection (LOD), excellent reproducibility, multi-component detection, *etc.*, and is more widely used. However, such methods still face some problems, such as the often large investment in instruments and consumables, dependence on special personnel to operate, and difficulty in using them for on-site testing.<sup>3–5</sup> For samples with a short shelf life, such as seafood, vegetables and other fresh foods, that are brought back to the laboratory from sampling points for testing, there may be problems such as sample deterioration or loss, resulting in inaccurate test results. Therefore, point-of-care testing (POCT) has attracted increasing attention due to its features,

<sup>a</sup>School of Marine Science and Technology, Harbin Institute of Technology (Weihai), Weihai 264209, China

<sup>b</sup>CAS Key Laboratory of Coastal Environmental Processes and Ecological Remediation, Shandong Key Laboratory of Coastal Environmental Processes, Shandong Research Center for Coastal Environmental Engineering and Technology, Yantai Institute of Coastal Zone Research, Chinese Academy of Sciences, Yantai 264003, China. E-mail: jhli@yic.ac.cn

<sup>c</sup>College of Chemistry and Chemical Engineering, Yantai University, Yantai 264005, China

<sup>d</sup>Shaanxi Engineering Laboratory for Food Green Processing and Safety Control, College of Food Engineering and Nutritional Science, Shaanxi Normal University, Xi’an 710062, China

<sup>e</sup>School of Pharmacy, Binzhou Medical College, Yantai 264003, China

*i.e.*, performing at the sampling site and using portable analytical instruments to quickly obtain test results.<sup>6</sup> What's more, there is an increasing need for rapid detection technologies for environmental pollutants and food contaminants/nutrients. Sensor technologies play a paramount role in the rapid detection field.

Meanwhile, molecular imprinting technology (MIT) as an interdisciplinary technology,<sup>7</sup> which simulates the antigen-antibody specific binding principle to prepare molecularly imprinted polymers (MIPs) with specific recognition sites of template molecules,<sup>8–12</sup> has received increasing attention. And, molecular imprinting-based sensors are gaining popularity. As is well known, traditional chemical/biosensors usually have a single response signal output for detection. However, due to the possible interference from internal and external factors, such as the influence of the background signal, changes in the detection environment, load on the sensor substrate, operation, *etc.*, it is inevitable that low sensitivity and poor immunity will occur.<sup>13,14</sup> The multi-signal ratio mode has been developed, which offers built-in correction for the detection system and background signal interference, and shows high accuracy and reliability in the detection of various targets.<sup>15</sup> Therefore, the multi-signal ratio mode can effectively overcome the shortcomings of the single-response signal mode. Amongst the multi-signal ratio modes, the ratiometric fluorescence method is favored as it uses one fluorescence signal as the response signal for detection and the other as the reference.<sup>16</sup> The fluorescence reference remains unchanged or produces a change opposite to that of the response signal, minimizing signal fluctuations caused by changes in the background environment.<sup>16</sup> Li *et al.*<sup>17</sup> designed a ratiometric fluorescence method for sensitively detecting Hg<sup>2+</sup> and Fe<sup>3+</sup> in fish samples. Yang *et al.*<sup>15</sup> constructed a ternary emission fluorescence sensor for the accurate and sensitive determination of ascorbic acid (AA) and alkaline phosphatase in food and

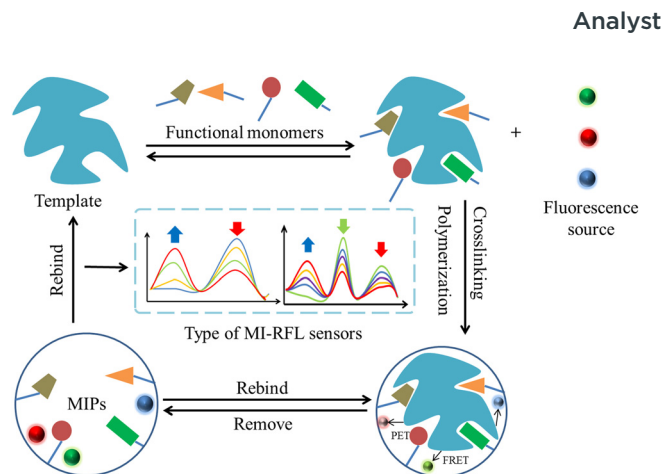


**Fig. 1** Schematic illustration of the basic construction and detection process of the MI-RFL sensor.

serum samples. Ratiometric fluorescence detection has been widely used in environmental and food analysis. However, the actual samples of the environment and food commonly have complicated matrices and the analytes are present in traces,<sup>2</sup> which requires high selectivity of sensors.

Therefore, introducing MIT in sensor construction can guarantee high selectivity of sensors. Combining the high selectivity of MIT recognition and ratiometric fluorescence detection technology, a molecular imprinting-based ratiometric fluorescence (MI-RFL) sensor has been constructed, with both high selectivity and high sensitivity. As schematically shown in Fig. 1, template molecules, fluorescence sources and functional monomers are reasonably selected, followed by crosslinking and polymerization. Then, MIPs are obtained after removing the template molecules. Upon rebinding the template with MIPs, the fluorescence source produces certain physicochemical changes for detection. Moreover, according to the number of emission peaks, the MI-RFL sensors are com-



**Yuhao Wen**

Yuhao Wen received his B.S. degree in Electrical Engineering and Automation from Heilongjiang University of Science and Technology in 2020. In 2021, he joined the Harbin Institute of Technology, jointly studying at the Yantai Institute of Coastal Zone Research, Chinese Academy of Sciences, as a master's degree candidate. His current research interest is focused on the construction and application of molecular

imprinting-based ratiometric fluorescence sensors and related microdevices.



**Jinhua Li**

Jinhua Li received her Ph.D. from Hong Kong Baptist University in 2009. In the same year, she joined the Yantai Institute of Coastal Zone Research, Chinese Academy of Sciences, as an Assistant Professor, and then she was promoted to Professor in 2021. Her current research focuses on molecular imprinting-based sample pretreatment and chemical/biological sensing analysis of contaminants in complicated samples. She has proposed

new construction strategies and application aspects of a series of molecular imprinting-based fluorescence sensors. As a major author, she has published over 140 SCI journal papers which have been cited more than 11 000 times and her H-index is 60.

monly divided into two major types, double and triple-emission sensors. The acquired sensors possess the advantages of both MIT and RFL, such as fantastic selectivity and sensitivity, non-destruction, rapidity, convenience, much easier visualization, *etc.* Sensors are drawing growing attention especially in environmental and food analysis. For example, Hu *et al.*<sup>18</sup> constructed a MI-RFL sensor based on a boric acid functionalized lanthanum metal–organic skeleton coupled with MIPs for the detection of ribavirin in eggs and water. Fu *et al.*<sup>19</sup> constructed a ternary-emission MI-RFL sensor to detect thiamphenicol in fish, shrimp, beef and milk samples. A systematic comparison of the advantages and limitations of the MI-RFL sensing method with other detection methods based on MIT is listed in Table 1.<sup>11,20–32</sup> As can be seen, MI-RFL sensors have unique superiority especially in the rapid and visual detection field.

Therefore, herein, we propose to review the recent advances in MI-RFL sensors for environmental and food analysis, focusing on construction and applications. To start with, various fluorescence sources and working principles are summarized. Then, new preparation techniques for MIPs including nanoimprinting technology, dummy imprinting strategy and so on are highlighted. Also, dual and ternary-emission types of MI-RFL sensors are emphasized. Subsequently, the analytical applications of MI-RFL sensors in the environmental and food fields are overviewed. Finally, we make some attempts to propose the challenges and development trends of MI-RFL sensors. We believe that MI-RFL sensors can provide influential platforms for rapid and precise target detection. We anticipate that the present review will play a good guiding role in grasping the development trends of MIT, RFL sensors, nanotechnologies, *etc.* and establish innovative research, as well as have important reference value for related researchers and governmental personnel/the public engaged in environmental protection and food safety.

## 2. Fluorescence sources and working principles of MI-RFL sensors

MI-RFL sensors produce fluorescence response signals and reference signals. Furthermore, the resulting fluorescence spectrum contains two or more emission peaks at a specific excitation wavelength.<sup>33</sup> The ratio of peak intensity is calculated as the output response of the MI-RFL sensor and a certain relationship is obtained between the ratio values and target's concentrations. Therefore, for constructing a MI-RFL sensor, fluorescence sources are firstly considered and then quantitative determination is carried out by utilizing the working principles.

### 2.1. Fluorescence sources

The essence of the ratiometric fluorescence method is using a fluorescence source to generate two or more response signals, and at the same time, at least one signal changes linearly with concentration.<sup>34,35</sup> Therefore, it is very critical to select a suitable fluorescence source during the construction of MI-RFL sensors. Currently, common fluorescent materials for MI-RFL sensors include fluorescent dyes,<sup>36</sup> fluorescent nanoparticles<sup>37–39</sup> and fluorescent targets.<sup>40</sup> Their advantages and disadvantages are listed in Table 2.<sup>33,38–47</sup>

**2.1.1. Fluorescent dyes.** Fluorescent dyes are dyes that emit fluorescence after absorbing a certain wavelength of light, most of which are heterocyclic compounds containing benzene rings or conjugated bonds.<sup>48,49</sup> Due to the advantages of high sensitivity, excellent light stability and simple operation, fluorescent dyes are widely used in biological imaging, optical diagnosis and treatment and fluorescent probes. For example, Wang *et al.*<sup>50</sup> used nitrobenzoxadiazole (NBD) as fluorescence signal sources and the sol–gel polymerization

**Table 1** Comparison of MI-RFL sensing method with other detection methods based MIT

| Detection method            | Advantage   | Limitation   | Ref.               |
|-----------------------------|---|--|--------------------|
| MI-RFL sensor               | Recognition selectivity, high detection sensitivity, non-destruction, rapidity, application universality, visualization accuracy, device portability and easy on-site detection | The application range needs to be further improved, and the detection of gas is still blank.   | The present method |
| MI-FL sensor                | Simpler and easier fabrication  | Low anti-interference ability and low sensitivity  | 11 and 32          |
| MI-SERS sensor              | Unique features of fingerprint recognition, nondestructive property, high sensitivity, and rapidity   | Instrumentation is expensive, complex to operate, and substrate unstable   | 28–31              |
| MI-QCM sensor               | Specifically identify analytes of interest to improve selectivity and sensitivity   | Poor anti-interference and low accuracy  | 20 and 21          |
| MI-EC sensor                | Good repeatability and accuracy, low power consumption and good resolution  | Short service life   | 22 and 23          |
| MI-SPR sensor               | Real-time monitoring, label-free, high selectivity and sensitivity, and high throughput   | High detection cost, low stability, and low detection efficiency   | 24 and 25          |
| MI-SPE coupled with HPLC-MS | High throughput, high selectivity, high sensitivity, good durability and wide practicality  | The sample-pretreatment procedure is time/reagent consuming, instrument is relatively expensive and complicated, the total analysis process is long and it is difficult to carry out on-site detection | 26 and 27          |

FL: fluorescence; SERS: surface enhanced Raman scattering; QCM: quartz crystal microbalance; EC: electrochemistry; SPR: surface plasmon resonance; SPE: solid-phase extraction.

**Table 2** The advantages and disadvantages of different fluorescence sources used for the construction of MI-RFL sensors

| Fluorescence source       | Type     | Advantage  | Disadvantage   | Ref.      |
|---------------------------|----------|--|--|-----------|
| Fluorescence dyes         | NBD      | High sensitivity, good light stability, simple operation, and usually used   | Low signal-to-noise ratio, poor anti-interference, high toxicity                                     | 40        |
| Fluorescent nanoparticles | QDs      | High fluorescence yield, narrow emission spectrum, good symmetry, good photostability, good biocompatibility, spectral tunability and usually used | Strong toxicity  | 38 and 39 |
|                           | CDs      | Good biocompatibility, low toxicity, cheap availability of raw materials and sometimes used  | Poor stability, low quantum yield, and uneven distribution of luminescence wavelengths               | 41–43     |
|                           | MNCs     | Strong luminescence performance, good light stability and good biocompatibility  | Poor stability and seldom used   | 44        |
|                           | UCNPs    | Low toxicity, high chemical stability, excellent photostability, narrow emission band and long luminous life                                       | Particle agglomeration, low luminous efficiency caused by high-energy surface states and seldom used | 33        |
| MOFs                      | BA-LMOFs | High subject–object responsiveness and sometimes used  | The study of luminous performance is relatively weak   | 45 and 46 |
| Fluorescent targets       | FA       | Easy operation and sometimes used  | —  | 47        |

“—” indicates “none”; NBD: nitrobenzoxadiazole; QDs: quantum dots; CDs: carbon dots; MNCs: metallic nanoclusters; UCNPs: upconverting nanoparticles; MOFs: metal organic frameworks; BA-LMOFs: boric acid-functionalized lanthanide metal–organic frameworks; FA: folic acid.

process to prepare MI-RFL sensors for highly selective and highly sensitive detection of phycoerythrin (PE).

**2.1.2. Fluorescent nanoparticles.** Fluorescent nanoparticles are mainly composed of a matrix and an activator, and have the characteristics of strong absorption capacities, high conversion rates and stable physical and chemical properties.<sup>37</sup> At present, the most commonly used fluorescent nanoparticles for MI-RFL sensors are quantum dots (QDs). QDs possess the advantages of stable physicochemical properties, excellent biocompatibility, dispersion and simple surface functionalization.<sup>39</sup> In summary, QDs have been widely used. Arslan *et al.*<sup>51</sup> used QDs as the fluorescence source to construct a MI-RFL sensor to detect malachite green (MG). Amiri *et al.*<sup>52</sup> used QDs as the fluorescence source to prepare a MI-RFL sensor for the highly sensitive and selective determination of cytochrome c. Although QDs possess wide application prospects, their toxicity cannot be ignored. In order to solve this problem, carbon dots (CDs) have been gradually entering researchers' thinking. CDs possess numerous advantages like simple preparation, low cost, environmental friendliness, high quantum yield, low cytotoxicity, and marvelous biocompatibility.<sup>42,43,53</sup> Liu *et al.*<sup>54</sup> constructed a MI-RFL sensor, which functioned by FRET between photoluminescent CDs and 4-nitrophenol (4-NP), to detect 4-NP in water samples. Fu *et al.*<sup>55</sup> used CDs as fluorescence sources and constructed MI-RFL sensors for detecting phycoerythrin (PE). Additionally, metallic nanoclusters (MNCs) are another common source of fluorescence, and consist of several to hundreds of metal atoms, usually ranging in size from 1 to 10 nm.<sup>44</sup> MNCs exert special quantum size effects. Therefore, they exhibit superb light stability, low toxicity, Stokes displacement, no flickering, high catalytic activities, and antibacterial properties.<sup>56</sup> Lu *et al.*<sup>57</sup> used gold nanoparticles (AuNCs) as the fluorescence source and constructed a MI-RFL sensor

using double-emitting nanoparticles to detect bisphenol A (BPA).

**2.1.3. Fluorescent targets.** In addition to some of the commonly used fluorescent sources mentioned above, some of the analytes themselves also possess fluorescence. Therefore, when measuring such substances, only one more fluorescent source needs to be added. The concentration of the analyte can be measured by calculating the ratio of the fluorescence of the analyte itself to the introduced reference signal.<sup>16</sup> For example, Li *et al.*<sup>58</sup> developed MI-RFL sensors for ratiometric fluorescence and visual detection of folic acid (FA). As FA itself has fluorescence, the imprinting shell was anchored to the SiO<sub>2</sub> nanoparticles and CdTe QDs were embedded into the imprinting shell to provide FA-dependent fluorescence signals.

## 2.2. Working principles of MI-RFL sensors

During the working process of the sensor, the imprinted cavity in the MIPs specifically binds to the target, which can cause physicochemical changes in the fluorescence sources. There are four main working principles: fluorescence resonance energy transfer (FRET), photoinduced electron transfer (PET), aggregation-induced emission (AIE) and inner filter effect (IFE).

**2.2.1. Fluorescence resonance energy transfer.** FRET means that in two different fluorophores, if the emission spectrum of one fluorophore (donor) overlaps with the absorption spectrum of another group (acceptor), when the distance between these two fluorophores is appropriate, the phenomenon of fluorescence energy transfer from the donor to the acceptor can be observed, that is, when the acceptor is excited at the excitation wavelength of the donor, the fluorescence emitted by the acceptor can be observed.<sup>59</sup> Yang *et al.*<sup>60</sup> constructed a MI-RFL sensor and visually detected Brilliant Blue by the FRET mechanism. This MI-RFL sensor based on dual-

emission color controllable nanoparticles provides a new idea for highly selective, sensitive, fast and visual detection of colored substances in complex matrices.

**2.2.2. Photoinduced electron transfer.** A typical PET system is composed of an acceptor part containing an electron donor, which is connected to a fluorophore by a spacer.<sup>61</sup> In such a system, the fluorophore part is the place for absorbing light energy and emitting fluorescence, and the acceptor part is used to bind the guest; these two parts are separated by spacer groups, and connected to a molecule by spacer groups, forming a supramolecular system that selectively recognizes acceptors while leading to changes in light signals.<sup>32</sup> Wang *et al.*<sup>62</sup> fabricated a novel MI-RFL sensor for the detection of 2,4-dichlorophenoxyacetic acid (2,4-D) based on PET. This simple, fast and reliable visual sensing strategy offers potential applications for highly selective ultra-trace analysis of complex matrices.

**2.2.3. Aggregation-induced emission.** Traditional organic dyes typically have aggregation-induced quenching effects in the solid state, which makes most organic dyes unsuitable for use with MIPs. AIE may be a better candidate for the fluorescence signal portion of MIP-based fluorescence sensors due to their excellent luminescence properties in the aggregated state and solid state.<sup>63</sup> At the same time, AIE can be specially designed and functionalized to obtain high fluorescence quantum yields and good photobleaching resistance.<sup>63</sup> They have been introduced into many polymer fluorescence sensors and show excellent fluorescence performance.

**2.2.4. Inner filter effect.** The IFE has two meanings. First, in emission experiments, it refers to the significant reduction in quantum efficiency due to the reabsorption of radiation by the system itself, which is the band distortion effect.<sup>45</sup> Secondly, in experiments with light irradiation, the absorption of incident light by other components of the system is also known as the IFE.<sup>45</sup>

### 3. New techniques for MIP preparation in MI-RFL sensors

The preparation MIPs mainly uses free radical polymerization and sol-gel polymerization. Besides the polymerization methods, some new imprinting techniques have been developed for improving the performance of MIPs. As illustrated in Fig. 2, three technologies including surface imprinting, nanoimprinting and living/controlled radical polymerization (LCRP), and three strategies including dummy template, stimulus response imprinting and multi-functional monomer imprinting, are mainly utilized to promote the analytical performances of MI-RFL sensors.

#### 3.1. Surface imprinting technology

Surface imprinting technology prepares imprinted materials by controlling the positioning of templates on or near the surface of the material to create more efficient identification sites.<sup>64</sup> Its biggest feature is that it leads to the complete

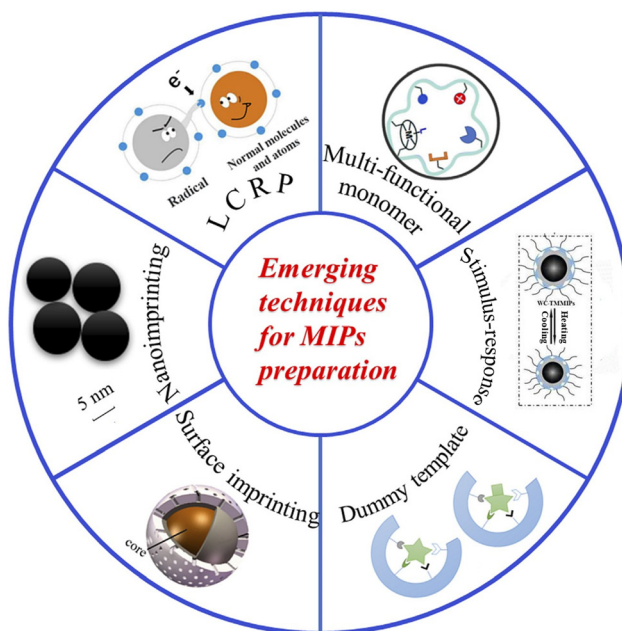


Fig. 2 Schematic diagram of the new typical techniques for MIPs preparation.<sup>26</sup>

removal of template molecules. Shell thicknesses that are too large are not conducive to sensitive analyte determination, and too small shell thicknesses may cause template leakage. Therefore, in the process of preparing MIPs, it is very necessary to select the appropriate shell thickness. The factors affecting the thickness of the shell generally include the polymerization method, imprinting time, crosslinker dosage, *etc.* Wang *et al.*<sup>65</sup> used TEOS self-polymerization for surface imprinting, and constructed a MI-RFL sensor for the detection of hepatitis B virus. Surface imprinting technology allows the template molecules to be completely removed, which greatly improves the sensor's anti-interference ability.

#### 3.2. Nanoimprinting technology

Nanoimprinting technology is used in the preparation of nanostructured MIPs, which has the advantages of high resolution, fast processing speed, high throughput, wide compatibility with materials and low cost, and is suitable for large-scale production of antibacterial surfaces based on a variety of polymer surfaces.<sup>66,67</sup>

#### 3.3. Living/controlled radical polymerization technology

LCRP with multiple advantages is a new polymerization method that has received widespread attention in the field of polymer synthesis, and this technology has penetrated into many fields such as medical products, nanomaterials and aerospace devices. Not only does it possess the advantage that it enables controlling the molecular weight of the polymer but also that it makes the polymer have a narrower molecular weight distribution. Also, it can realize end group functionalization, a three-dimensional structure, block copolymers and

grafted copolymers.<sup>68</sup> Li *et al.*<sup>69</sup> used QDs as a fluorescence source and atom transfer radical polymerization to construct a dual-emission MI-RFL sensor for detecting 2,4-D in pure milk. The sensor has exceptional photostability and reusability, high 2,4-D selectivity and sensitivity, and direct visual detection capabilities in pure milk.

### 3.4. Dummy imprinting strategy

The dummy imprinting strategy for wider analytes refers to the synthesis of MIPs from a substance similar to the target molecular structure as a template molecule, that is, dummy template MIPs, which can effectively avoid the influence of template leakage on the detection results and improve the accuracy of analysis.<sup>70</sup> Qi *et al.*<sup>71</sup> used monensin as a fragment dummy template molecule and constructed a MI-RFL sensor for the detection of the ciguatera toxin P-CTX-3C.

### 3.5. Stimulus-response imprinting strategy

Stimulus-responsive polymers are polymers whose physical or chemical properties change as the external environment changes. With rapid development of detection and monitoring technologies driven by the needs of various industries in society, researchers have put forward more intelligent, high-throughput and high-sensitivity requirements for MIPs, and stimulus-responsive molecularly imprinted polymers (SR-MIPs) came into being.<sup>72</sup> Li *et al.*<sup>73</sup> used QDs as fluorescent sources, *N*-isopropylacrylamide as heat-responsive functional monomers, *N,N*-methylene bis-acrylamide as cross-linking agents, and PC as templates to prepare MI-RFL sensors by simple and easy polymerization. This study provides a simple, rapid and intelligent method for the identification and analysis of trace proteins in complex water matrices, which has promoted the study of stimulus-response imprinting.

### 3.6. Multi-functional monomer imprinting strategy

The multi-functional monomer imprinting strategy improves the non-covalent binding between target molecules and functional monomers by using more than two functional monomers to interact with template molecules. The use of multi-functional monomers is a good choice to improve the adsorption and selectivity of MIPs.<sup>74</sup> Wang *et al.*<sup>74</sup> prepared green ion-imprinted polymers in the aqueous phase by synergistic action of three functional monomers, low-cost environmentally friendly gelatin, 8-hydroxyquinoline and chitosan, and removed copper ions from the aqueous solution.

## 4. Fluorescence emission types of MI-RFL sensors

Compared with single-emission fluorescence sensors, the ratiometric type can provide more sensitive and accurate quantification and a better visualization effect. Nowadays, MI-RFL sensors include both dual-emission and triple-emission types. At the moment, the most common type is dual emission. As the name suggests, dual emission means that the

sensor has two emission peaks, one of which is the response signal and the other is the reference signal, and the ratio of the reference signal to the response signal is the output response of the sensor.<sup>75</sup> The output response of the sensor is linearly related to the number of molecules to be measured within a certain range. MI-RFL sensors can be divided into two categories depending on the type of reference signals: one is that if the analyte of interest has been identified, the fluorescence intensity of one emission peak will change. Lu *et al.*<sup>76</sup> constructed a MI-RFL sensor to detect BPA in river water by simultaneously anchoring QDs to MIPs using post-imprinting of modification (PIMod) strategies. The process for the preparation of MIPs *via* the doping method and PIMod method is shown in Fig. 3A. As the BPA concentration increases, the fluorescence intensity of the QDs gradually decreases and is eventually completely quenched. The other type of dual emission sensor usually embeds an inert fluorophore as a reference in a mesoporous silicon material, while another target-sensitive fluorophore is grafted at the imprinting level.<sup>77</sup> As the concentration of the molecule of interest increases, the fluorescence intensity of the sensitive fluorophore changes, while the reference fluorescence intensity does not change. Li *et al.*<sup>78</sup> constructed a MI-RFL sensor for the highly sensitive and selective detection of 4-NP, using CDs as the sensitive fluorophore and YVO<sub>4</sub>:Eu<sup>3+</sup> nanoparticles as the reference fluorophore.

Compared with dual-emission modes, triple-emission MI-RFL sensors provide more accurate results, higher sensitivity and better visualization. Yang *et al.*<sup>79</sup> used three-color fluorescence sources to prepare MIPs in three colors, and then mixed the three MIPs in the appropriate proportions to construct a three-emission MI-RFL sensor for visual detection of bovine hemoglobin (BHb), as schematically illustrated in Fig. 3B. This post-imprinting mixing (PIMix) method is universal and can be extended to environmental and food samples. The triple-emission MI-RFL sensors need to be vigorously worked, and PIMix and PIMod are ideal construction strategies.<sup>16</sup> At the same time, the triple-emission system can be designed by using the fluorescence of the target to prepare MI-RFL sensors as the template, which can further simplify the sensor construction process.<sup>47</sup>

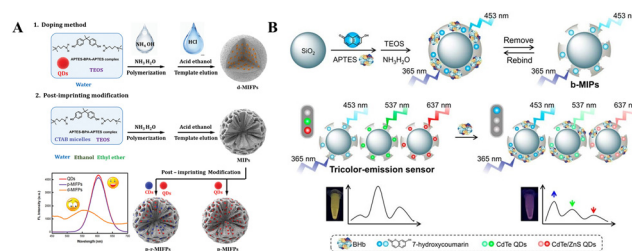


**Fig. 3** Post-imprinting strategies. (A) Process for the preparation of MIPs *via* the doping method and post-imprinting modification method.<sup>76</sup> (B) Schematic illustration for the preparation of blue-emission MIPs (b-MIPs) and the construction of a triple-color emission sensor by mixing blue-, green- and red-emission MIPs (b-, g-, and r-MIPs) at an optimized volume ratio of 50/110/60.<sup>79</sup>

## 5. Applications to environmental and food analysis

MI-RFL sensors combine the specific recognition of MIT with the immunity of ratiometric fluorescence.<sup>11</sup> Therefore, it possesses very excellent performance, suitable for complex environmental and food analysis. Some typical application examples of MI-RFL sensors are listed in Table 3.<sup>18,19,47,50,55,57,58,60,62,71,73,76,78,80–104</sup> There is no doubt that MI-RFL sensors are on a rapidly evolving trajectory and enjoy significant advantages and diverse applications.

### 5.1. Environmental analysis

Environmental analysis is the basis for the scientific management of the environment and supervision of environmental law enforcement. The core task is to determine environmental pollutants. It is an indispensable basic work for environmental protection. Now, new pollutants<sup>105</sup> are becoming a research hotspot along with the continuous research on other pollutants.<sup>106</sup>

**5.1.1. New pollutants.** New pollutants are also known as “emerging pollutants” or “new contaminants”. With the large-scale use of various chemicals, the harm of new pollutants such as endocrine disrupting chemicals (EDCs), new persistent organic pollutants, microplastics and antibiotics to the ecological environment and human health is gradually emerging and becoming more and more serious.<sup>107</sup> Analytical determination studies of new pollutants play important roles in the environmental management of chemicals to prevent the risk of new pollutants.

EDCs are toxic chemicals that are found in the environment and cause hormonal-like effects on animals, including humans.<sup>108</sup> We may come into contact with endocrine disruptors through food, drinking water and inhalation of air pollutants, or through our skin. You *et al.*<sup>98</sup> prepared ternary-emission MI-RFL sensors by mixing blue and red emitting QDs with green QDs in optimal proportions for the detection of dibutyl phthalate (DBP) in seawater and aquatic products. Fig. 4A shows the sensor construction and detection process. The ratiometric fluorescence value of the sensor changed linearly in the concentration range of 2.0–20.0 mg L<sup>-1</sup>. The LOD in fish and seawater was 1.0 µg kg<sup>-1</sup> and 0.65 µg L<sup>-1</sup>, respectively. The recovery rates of DBP in fish and seawater are 84.3%–91.4% and 88.3%–110.3%, respectively. This sensor provides an ideal choice for fast and intuitive detection of DBP in the environment and aquatic products.

In recent years, the irrational use of antibiotics has led to increasingly serious environmental pollution.<sup>26,109</sup> Since the advent of penicillin, antibiotics have been produced and used in large quantities. The misuse and improper discharge of antibiotics has led to an increase in bacterial resistance, leading to outbreaks of superbugs.<sup>110</sup> Therefore, it is of great significance to develop MI-RFL sensors for rapid detection of antibiotics in the environment. Ma *et al.*<sup>100</sup> constructed a MI-RFL sensor for the simultaneous detection of complexes of

streptomycin sulfate (SS) and kanamycin sulfate (KS). This sensor is used to detect SS with concentrations ranging from 3.00 to 118 mM and KS ranging from 3.00 to 105 mM with LOD of 0.22 mM and 0.24 mM, respectively. Through quantitative analysis of SS core KS in river water samples, marvelous recovery rates are obtained, indicating that it is feasible for sensors to detect antibiotics in water samples. Wu *et al.*<sup>97</sup> constructed a MI-RFL sensor and used it to achieve selective and accurate detection of norfloxacin (NOR). The preparative strategy of CdTe@SiO<sub>2</sub>@fluorescence MIPs (FMIPs) for the detection of NOR is shown in Fig. 4B. The CdTe QDs encapsulated in SiO<sub>2</sub> serve as reference signals, and CDs doped in the imprint layer serve as response signals. Under the optimal conditions, NOR rapidly boosted CdTe@SiO<sub>2</sub>@FMIPs at 435 nm for 1 min and showed a good linear relationship between fluorescence enhancement efficiency and NOR concentration above 10–90 nM, with the LOD of 3.28 nM. Through actual sample, such as lake water, tap water and unfiltered lake water, experiments, the recovery values were 93.4%–107.7% and the relative standard deviation (RSD) was 2.0%–3.6%. Hu *et al.*<sup>80</sup> constructed a MI-RFL sensor by using surface imprinting technology for MIP preparation, and applied it to detect oxytetracycline (OTC) in water and milk. In order to achieve accurate analysis in the field, a portable intelligent sensing platform was designed by smartphone auxiliary devices. The smartphone is equipped with a color recognizer app as a signal reader and analyzer to enable OTC visual sensing by capturing and digitizing fluorescence images. What's more, the portable platform was successfully applied to on-site monitoring of OTC in water and milk samples with satisfactory results. The schematic diagram of using the developed smartphone-integrated sensing platform to detect OTC is shown in Fig. 4C. As a result, the platform under development shows low cost, portability, ease of implementation, ideal specificity, and sensitivity, offering great potential for POCT.

**5.1.2. Other environmental pollutants.** At present, the pollution caused by traditional pollutants mainly includes air pollution, soil pollution and water pollution. Among them, due to the strong fluidity and deformation of gases, there are currently very few gas sensors. The research on water pollution and soil pollution is relatively mature.

Water is the source of life, yet the quality of water has deteriorated due to urbanization, rapid population growth, pollution from agricultural activities and industrial development.<sup>111</sup> What's more, about 71% of the Earth's surface is covered by water, so the marine environment is supposed to be of concern and should be protected. Heavy metals, microbial pollutants and nutrients are the most common aspects of water quality research.<sup>111</sup> For example, currently, cyanobacteria blooms pose a significant threat to water bodies, aquatic animals and human health, as they may lead to water pollution, hypoxia, biodiversity loss and the production of toxic secondary metabolites.<sup>85</sup> PC is a pigment protein specific to cyanobacteria that, due to its close relationship to cyanobacteria biomass, typically provides quantitative information relevant to the assessment of cyanobacteria blooms.<sup>50</sup> Therefore,

Table 3 Applications of MI-REL sensors in environmental and food analysis

| Type                              | Fluorescence sources               | Analyte               | Functional monomer                  | Crosslinker                    | Polymerization method  | Working mechanism             | Imprinting strategy                         | Linear range  | LOD   | Real samples   | Recovery (%) | RSD (%) | Ref. |
|-----------------------------------|------------------------------------|-----------------------|-------------------------------------|--------------------------------|------------------------|-------------------------------|---|---|---|--|--------------|---------|------|
| Environmental analysis            | QDs, NBD                           | 2,4-D                 | APTES                               | TEOS                           | Sol-gel polymerization | PET                           | —   | 0.4–100 $\mu\text{M}$                                     | 0.14 $\mu\text{M}$                                | Lake water and tap water   | 95.0–110.1   | 4.5     | 62   |
|                                   | CDS, $\text{YVO}_4:\text{Eu}^{3+}$ | 4-NP                  | APTES                               | TEOS                           | Sol-gel polymerization | PET, FRET                     | —   | 0–12 $\mu\text{M}$  | 0.15 $\mu\text{M}$                                | Tap water and human urine  | 94.6–106.3   | <5.8    | 78   |
|                                   | NBD, PC                            | PC                    | APTES                               | TEOS                           | Sol-gel polymerization | FRET                          | —   | 0–250 nM  | 0.14 nM   | Seawater and lake water  | 93.8–110.2   | 4.7     | 50   |
|                                   | CDS, AuNCs                         | BPA                   | APTES                               | TEOS                           | Sol-gel polymerization | FRET                          | —   | 0.5–2.0 $\mu\text{M}$                                     | 29 nM   | Tap water and river water  | 95.9–98.9    | 3.9     | 57   |
|                                   | QDs                                | 2,4,6-Trinitrophenol  | APTES                               | TEOS                           | —                      | RET                           | Surface imprinting                          | 100–700 nM  | 43 nM   | Canned milk powder and canned fish<br>Deionized water, tap water,<br>mineral water and river water | 92.6–98.6    | 3.5     | 103  |
| QDs                               | PC                                 | N-Isopropylacrylamide | <i>N,N</i> -Methylene bisacrylamide | Simple facile copolymerization | FRET                   | Stimuli responsive imprinting | 0–1.8 $\mu\text{M}$                         | 3.2 nM  | Seawater  | 92.0–106.8   | 2.9–5.5      | 73      |      |
| QDs                               | MG                                 | APTES                 | TEOS                                | Copolymerization               | FRET                   | Surface imprinting            | 27.4 nM–137 $\mu\text{M}$                   | 17.0 nM   | Lake and river water                              | 95.8–107.3   | 0.01–1.19    | 102     |      |
| QDs                               | PC                                 | Dopamine              | TEOS                                | Self-polymerization            | —                      | —                             | 0.3–5.0 $\mu\text{M}$                       | 0.075 $\mu\text{M}$                                       | Seawater, lake water and bovine urine             | 90.8–110.1   | 4.6          | 101     |      |
| QDs                               | SS and KS                          | APTES                 | TEOS                                | Copolymerization               | ET                     | —                             | 3.00–108 $\mu\text{M}$                      | 0.22 $\mu\text{M}$  | River water                                       | 97.7–106.6   | 2.17–6.21    | 100     |      |
| CDS                               | PE                                 | APTES                 | TEOS                                | —                              | FRET                   | Surface imprinting            | 3.00–105 $\mu\text{M}$                      | 0.24 $\mu\text{M}$  | Real human serum,                                 | 102.5–112.6  | 1.12–3.85    | 55      |      |
| QDs                               | P-nitrophenol                      | F-PDA                 | EGDMA                               | Precipitation polymerization   | ET                     | —                             | 5–200 ng mL <sup>-1</sup>                   | 1.5 ng mL <sup>-1</sup>                                   | seawater and river water                          | 99.87–135.7  | 2.8–3.6      | 99      |      |
| QDs                               | DBP                                | APTES                 | TEOS                                | Reverse microemulsion          | PET                    | —                             | 0–10 000 nM                                 | 56.68 nM  | Drinking water and industrial wastewater          | 88.3–110.3   | <10.5        | 98      |      |
| QDs, CDS                          | NOR                                | MAA                   | EGDMA                               | Precipitation polymerization   | —                      | —                             | 2.0–20.0 $\times 10^3$ $\mu\text{g L}^{-1}$ | 0.65 $\mu\text{g L}^{-1}$                                 | Fish  | 84.3–91.4  | —            | 97      |      |
| QDs, CDS                          | BPA                                | APTES                 | TEOS                                | —                              | FRET                   | PIMod and surface imprinting  | 10–90 nM                                    | 3.28 nM   | Tap water, lake water and unfiltered lake water   | 93.4–107.7   | 2.0–3.6      | 76      |      |
| QDs                               | 4-NP                               | APTES                 | TEOS                                | Microemulsion polymerization   | ET                     | —                             | 0.005–4.0 $\mu\text{M}$                     | 0.57 nM   | River water                                       | 96.4–102.0   | <4.1         | 96      |      |
| CDS, FITC                         | MCS                                | APTES                 | TEOS                                | Sol-gel polymerization         | PET                    | Dummy imprinting              | 0.01–10 $\mu\text{M}$                       | 3.0 nM  | Huamei pool and electroplating factory wastewater | 91.0–103.9   | 1.7–4.9      | 95      |      |
| $\text{NH}_2\text{-MIL-101 (Fe)}$ | DA                                 | APTES                 | TEOS                                | Sol-gel polymerization         | —                      | —                             | 0.5–500 $\mu\text{g L}^{-1}$                | 0.013 $\mu\text{g L}^{-1}$ and 0.022 $\mu\text{g L}^{-1}$ | Binhai lake                                       | 104.72–108.14  | 2.83–4.91    | 94      |      |

Table 3 (Contd.)

| Type          | Fluorescence sources                          | Analyte        | Functional monomer | Crosslinker | Polymerization method        | Working mechanism      | Imprinting strategy          | Linear range                   | LOD  | Real samples   | Recovery (%) | RSD (%)   | Ref. |
|---------------|---|----------------|--------------------|-------------|------------------------------|------------------------|------------------------------|--------------------------------|--|--|--------------|-----------|------|
| Food analysis | QDs   | Melamine       | APTES              | TEOS        | Reverse micro-emulsion       | ET and charge transfer | —                            | 50–1000 ng mL <sup>-1</sup>    | 13 ng mL <sup>-1</sup>                     | Milk   | 94.1–98.7    | 3.6–5.1   | 93   |
|               | CDS   | Monensin       | APTES              | TEOS        | Sol-gel polymerization       | —                      | Dummy imprinting             | 0.001–1 ng mL <sup>-1</sup>    | 3.3 × 10 <sup>-4</sup> ng mL <sup>-1</sup> | Eel, bass, and grouper   | 80.00–91.33  | <9.91     | 71   |
|               | QDs   | Sulfadiazine   | APTES              | TEOS        | —                            | —                      | Surface imprinting           | 0.25–20 μM                     | 0.042 μM                                   | Tap water and milk   | 79.3–101.2   | 9.56      | 92   |
|               | QDs   | TCS            | AM                 | EGDMA       | Precipitation polymerization | ET                     | —                            | 10–160 μM                      | 0.35 μM                                    | Milk   | 96.3–106.2   | <4.3      | 91   |
|               | AIE   | Rh 6G          | MAA                | EGDMA       | Precipitation polymerization | AIE                    | —                            | 0.0–10.0 μM                    | 0.26 μM                                    | Dried papaya and beverage  | 96.7–103.3   | 1.97–3.55 | 90   |
|               | QDs   | MG             | APTES              | TEOS        | Sol-gel polymerization       | FRET                   | —                            | 0.1–3.2 μM                     | 5.6 μg kg <sup>-1</sup>                    | Fish   | 94.3–110.2   | ≤2.3      | 89   |
|               | QDs   | Brilliant blue | APTES              | TEOS        | Sol-gel polymerization       | FRET                   | Surface imprinting           | 0–1.0 μM                       | 8.8 nM                                     | Carbonated beverage, brandy cocktail, popping candy, chocolate candy, mung bean cake and dried blueberry | —            | <3.5      | 60   |
|               | QDs   | FA             | APTES              | TEOS        | Sol-gel polymerization       | PET                    | Surface imprinting           | 0.23–113 μM                    | 48 nM                                      | Spinach, broccoli, tomato, and orange  | 94.8–104.2   | —         | 58   |
|               | QDs and NBD                                   | 2,4-D          | 4-VP               | EGDMA       | RAFT                         | —                      | —                            | 0–15 μM                        | 0.13 μM                                    | Milk   | 96.0–103.2   | 1.5–5.5   | 88   |
|               | QDs   | FA             | APTES              | TEOS        | Sol-gel polymerization       | PET                    | PIMix and surface imprinting | 0.01–50 ppm                    | 0.0052 ppm                                 | Milk powder, FA tablets and porcine serum  | 99.5–108.0   | <3.0      | 47   |
|               | QDs   | BHb            | APTES              | TEOS        | Sol-gel polymerization       | —                      | Surface imprinting           | 0.05–4 μM                      | 13 nM                                      | Bovine urine   | 96.2–103.8   | —         | 87   |
|               | QDs and NBD                                   | 2,4-D          | 4-VP               | EGDMA       | ATRP                         | —                      | Surface imprinting           | 0–50 μM                        | 0.13 μM                                    | Goat milk and pure bovine milk   | 97.9–104.5   | 1.2–6.0   | 86   |
|               | CDS, FITC                                     | OVA            | APTES              | TEOS        | Sol-gel polymerization       | FRET                   | Surface imprinting           | 0.05–2 μM                      | 15.4 nM                                    | Human urine  | 92.0–104.0   | 3.3–3.9   | 85   |
|               | QDs   | AA             | APTES              | TEOS        | —                            | —                      | —                            | 1–500 μM                       | 0.78 μM                                    | Chicken egg white  | 93.3–101.0   | 2.7–3.8   | 84   |
|               | QDs   | BHb            | APTES              | TEOS        | Sol-gel polymerization       | PET                    | PIMix                        | 0.025–3 μM                     | 7.8 nM                                     | Vitamin C tablets  | 96.0–99.0    | <1.7      | 84   |
|               | CDS   | BPA            | 4-VP               | EGDMA       | Precipitation polymerization | ET                     | —                            | 0–60 nM                        | 0.778 nM                                   | Bovine urine   | 99.25–111.7  | 1.8–3.2   | 79   |
|               | CDS   | pyrethroids    | APTES              | TEOS        | —                            | PET                    | Surface imprinting           | 1–150 μg L <sup>-1</sup>       | 0.048 μg L <sup>-1</sup>                   | Canned fish  | 96.58–102.04 | 3.11–4.38 | 83   |
|               | CDS   | TAP            | APTES              | TEOS        | One-pot self-polymerization  | PET                    | —                            | 5.0 nM–6.0 μM                  | 1.9 nM                                     | Tap water, tea, cucumber and apple   | 87.93–101.4  | 1.5–5.1   | 82   |
|               | luminescence metal organic framework and CdTe | CAP            | APTES              | TEOS        | Sol-gel polymerization       | PET                    | One-pot imprinting method    | 6.0–26.0 μM                    | 0.9 nM                                     | Fish, shrimp, beef and milk  | 95.0–105.0   | <5        | 19   |
|               | CDS   | OTC            | APTES              | TEOS        | Sol-gel polymerization       | IFE and AE             | Surface imprinting           | 10 pM–0.5 nM and 0.5 nM–4.5 nM | 3.8 pM                                     | Meat, milk and honey   | 98.2–101.2   | 2.4–3.6   | 81   |
|               | BA-LMOFs                                      | RBV            | MAA                | EGDMA       | —                            | —                      | Surface imprinting           | 0.02–50 μg mL <sup>-1</sup>    | 6.6 ng mL <sup>-1</sup>                    | Lake water and milk  | 90.58–96.79  | 1.1–3.3   | 80   |
|               | CDS   | CAP            | APTES              | TEOS        | Sol-gel polymerization       | ET                     | —                            | 2.5–1200 ng mL <sup>-1</sup>   | 7.62 ng mL <sup>-1</sup>                   | Lake water and egg   | 87.5–98.5    | 0.7–5.2   | 18   |
|               | CDS   | CAP            | APTES              | TEOS        | Sol-gel polymerization       | —                      | —                            | 0.1–3 μg L <sup>-1</sup>       | 0.035 μg L <sup>-1</sup>                   | Milk   | 96.5–106.6   | 1.1–3.5   | 104  |

“—” indicates “none”; LOD: limit of detection; QDs: quantum dots; NBD: nitrobenzoxadiazole; 2,4-D: 2,4-dichlorophenoxyacetic acid; APTES: 3-aminopropyltriethoxysilane; TEOS: tetraethyl orthosilicate; CDS: carbon dots; PET: photoinduced electron transfer; 4-NP: 4-nitrophenol; FRET: fluorescence resonance energy transfer; PC: phycoerythrin; AuNCs: gold nanoparticles; BPA: bisphenol A; RET: resonance energy transfer; MG: malachite green; SS: streptomycin sulphate; KS: kanamycin sulfate EGDMA: ethylene glycol dimethacrylate; DBP: dibutylphthalate; NOR: norfloxacin; ET: electron transfer; MCS: microcystins; DA: domoic acid; TCS: tetracycline; AM: acrylamide; AIE: aggregation-induced emission; Rh 6G: rhodamine 6G; FA: folic acid; 4-VP: 4-vinylpyridine; BHb: bovine hemoglobin; FITC: fluorescein isothiocyanate; OVA: ovalbumin; AA: ascorbic acid; TAP: thiampenicol; CAP: chloramphenicol; OTC: oxytetracycline; BA-LMOFs: boronic acid-functionalized lanthanide metal-organic frameworks; RBV: ribavirin; IFE: inner filter effect; AE: antenna effect; RAFT: reversible addition-fragmentation chain transfer; ATRP: atom transfer radical polymerization; MAA: methacrylic acid; F-PDA: fluorescent polydopamine; PE: phycoerythrin; PIMix: post imprinting of mixing; PIMod: post imprinting of modification.

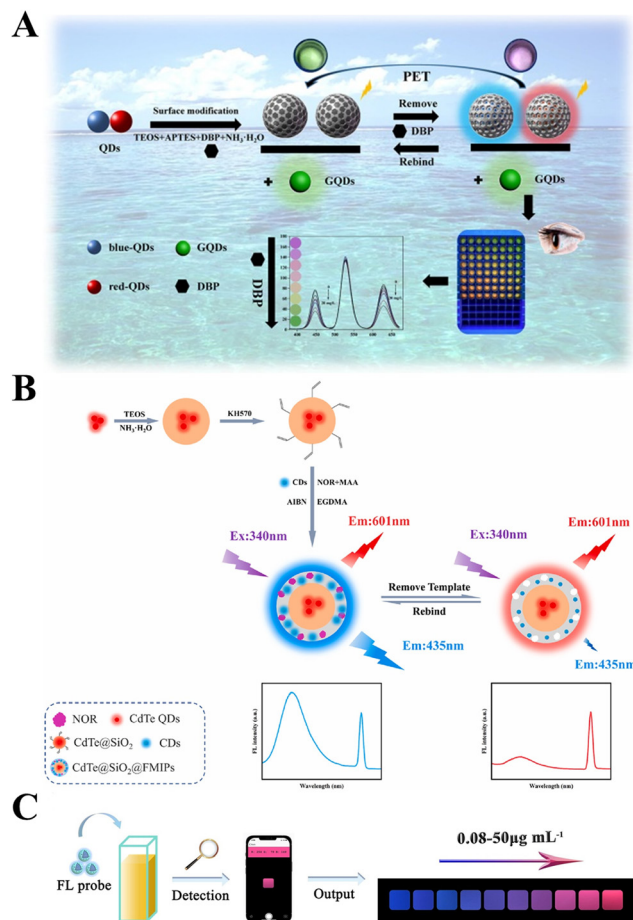


**Fig. 4** Schematic illustration of the MI-RFL sensors for the detection of new pollutants. (A) Sensor construction and detection process for DBP.<sup>98</sup> (B) Preparative strategy of CdTe@SiO<sub>2</sub>@FMIPs for the detection of NOR.<sup>97</sup> (C) The developed smartphone-integrated sensing platform to detect OTC.<sup>80</sup>

the PC in cyanobacteria can be used as an indicator of cyanobacteria and has key implications for marine environmental analysis. Furthermore, PC can emit fluorescence with high absorption coefficients over a wide spectral range, which has high biological and biomedical value and is stable in water for a long time. Therefore, it is urgent to develop sensitive, selective, fast, low-cost and environmentally friendly methods to identify and detect PC. Li *et al.*<sup>73</sup> developed a thermosensitive MI-RFL sensor by adopting stimuli-responsive imprinting and multi-functional monomer imprinting strategies for detecting PC in seawater. QDs were used as the fluorescence source, and the ratio of the emission intensity of QDs to PC was used to determine the contents of PC. The sensor achieved a good linear relationship ranging from 0 to 1.8 μM with a low LOD of 3.2 nM. Satisfactory recoveries within 92.0%–106.8% were attained in seawater samples. This study provides a simple, fast and intelligent method for the identification and analysis of PC in complex environmental water. Wang *et al.*<sup>50</sup> designed a simple strategy to fabricate a MI-RFL sensor following MIP preparation *via* surface imprinting for highly selective and sen-

sitive detection of PC using NBD as the fluorescence signal source through a sol-gel polymerization process. The LOD was as low as 0.14 nM, and with a better recognition specificity for PC than its analogues with a high imprinting factor of 9.1. In addition, the sensor showed high recoveries of 93.8%–110.2% and a high accuracy with RSDs less than 4.7% in seawater and lake water samples.

At present, due to the uncontrollable effect of the atmosphere and water on the soil, as well as a large number of human activities, soil pollution is becoming increasingly serious. For example, the irrational use of pesticides is receiving increasing attention. Global surveys document the pollution and impacts of pesticide residues on soil, terrestrial and aquatic ecosystems, including coastal marine systems and their toxic effects on human and non-human biota.<sup>2,112,113</sup> Wang *et al.*<sup>62</sup> used a sol-gel method to construct a MI-RFL sensor for detecting 2,4-D. With this sensor, a continuous color change from orange-red to green can be observed with the naked eye. This sensor obtained a high sensitivity with the LOD of 0.14 μM within 5 min, and the recognition selectivity for 2,4-D was better than for its analogue. This sensor was successfully applied to the determination of 2,4-D in actual water samples, with high recoveries from 95.0% to 110.1% and a high precision with RSDs less than 4.5%. Such simple, fast and reliable visual sensing strategies not only provide potential applications for highly selective ultra-trace analysis of complex matrices, but also greatly enrich the research dimensions of MI-RFL sensors.

## 5.2. Food analysis

Food safety is an interdisciplinary field that specializes in ensuring food sanitation and safety for edible use, reducing hidden dangers of disease, and preventing food poisoning in the process of food processing, storage, and sales.<sup>114</sup> Therefore, it is highly critical to maintain food safety. The planting, breeding, processing, packaging, storage, transportation, sales, consumption and other activities of food comply with the mandatory standards and requirements of the state, and there is no hidden danger that may damage or threaten human health to cause consumers to die or endanger consumers and their descendants.<sup>115</sup> The concept shows that food safety includes both production safety and business safety; this includes both product safety and process safety; this includes both security in the present and security in the future.

The essential aspect of ensuring food safety is testing the composition of the foods. When the content any component is too low, nutrition from that component in the food is not guaranteed. For example, FA is one of the essential vitamins for the growth and reproduction of the body's cells. If it is lacking, it has an impact on the normal physiological activities of the human body, and can even produce anemia, tumors and other diseases. People often consume substances such as vegetables and milk powder to supplement FA. Li *et al.*<sup>58</sup> designed a dual-emission MI-RFL sensor by using surface imprinting technology and the PIMix method for the detection

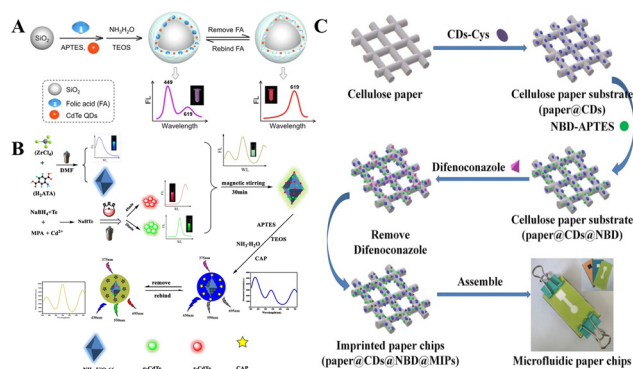


**Fig. 5** Application of MI-RFL sensors in food analysis (A) schematic illustration for the one-pot preparation process of nanoscale core-shell structured FA imprinted ratiometric fluorescence sensor and possible detection principle.<sup>58</sup> (B) Preparation and detection procedure of ternary-emission MOF@g-CdTe@r-CdTe@MIP.<sup>81</sup> (C) Construction of MIP-based ratiometric fluorescent microfluidic paper chip.<sup>117</sup>

of FA in milk powder and FA tablets. The sensor's construction and detection process are shown in Fig. 5A. Under the optimal conditions, the fluorescence intensity ratio ( $I_{449}/I_{619}$ ) had a good linearity with the FA concentration of 0.23–113  $\mu\text{M}$ . The LOD was 48 nM. When used for detecting real samples, the sensor exhibited excellent sensing properties such as fast response, high accuracy, high sensitivity, and selective identification. Furthermore, a ternary-emission MI-RFL sensor for FA detection was constructed by Yang *et al.*,<sup>47</sup> based on the PIMix method and surface imprinting. Under optimal conditions, within the concentration range of 0.01–50 ppm, the ratio intensity of the three-color emission changed in a logistic function, corresponding to the fluorescent color change from yellow to orange, red to violet, and finally to blue. The sensor successfully measured FA in complex food and serum samples with results comparable to the PRC standard methods.

Another aspect of ensuring food safety is the monitoring and removal of harmful substances from food. For example, in order to improve the taste and extend the shelf life of food, additives are widely used in food. Food additives promote the development of the food industry and are known as the soul of the modern food industry, mainly due to the host of benefits they bring to the food industry. Their main role is to prevent food spoilage, improve the sensory quality of food, maintain nutritional value and facilitate food supply or processing.<sup>116</sup> However, the misuse of food additives has also caused much harm. The irrational use of food additives may lead to the loss of nutrition and cause damage to human health. Therefore, the rational use of food additives is an imperative aspect of ensuring food safety. Yang *et al.*<sup>60</sup> used surface imprinting technology combined with single-component dual-emission nanoparticles to construct a dual-emission MI-RFL sensor for detecting Brilliant Blue in food *via* the FRET mechanism. This sensor offered a good linear relationship in the range of 0–1.0  $\mu\text{M}$ , with the LOD up to as low as 8.8 nM. The results of the detection of Brilliant Blue in food samples were consistent

with that obtained by the conventional methods, and the RSDs were less than 3.5%. Therefore, this sensor provided a simple effective method to detect Brilliant Blue in food. Wu *et al.*<sup>81</sup> combined luminescent metal-organic frameworks (MOFs), green CdTe and near-infrared red CdTe to develop a ternary-emitting MI-RFL sensor *via* sol-gel polymerization and one-pot imprinting, for visual detection of chloramphenicol (CAP) in food. Fig. 5B schematically shows the sensor's construction and detection processes. Good linear relationships in the concentration range of 10 pM–0.5 nM and 0.5 nM–4.5 nM, were attained, with a fast response time of 3 minutes. The LOD of CAP was 3.8 pM. This sensor offered richer color variations, from yellow–green to apricot to orange–salmon to amaranth to purple to finally blue. When applied to the detection of trace CAP in food, high recoveries within 98.2%–101.2% were obtained, indicating practical applicability for the rapid visual detection of CAP. Ma *et al.*<sup>117</sup> constructed a MI-RFL sensor and designed a microfluidic paper chip for the rapid visual detection of difenoconazole in tomatoes. The construction process of microfluidic chips is shown in Fig. 5C. Under the optimized conditions, the linearity range of the fluorescence sensor was 0.3–60  $\mu\text{M}$ , with the LOD up to as low as 75 nM, the sample recovery values were 102.1%–111.2%, and the RSDs were 3.1%–4.2%. Compared with traditional liquid fluorescence sensing materials, such solid-phase matrix sensors possess several advantages including better portability and storage, and satisfactory fluorescence detection characteristics. Additionally, this sensor had high specificity for the separation and detection of difenoconazole, and was successfully applied to the detection of tomato samples. This study opened up a new way for the combination of novel ratiometric fluorescence technology and microfluidic paper-based chips.

## 6. Conclusions and perspectives

As mentioned above, the MI-RFL sensors combining MIT and ratiometric fluorescence have proved to be powerful platforms for precise target detection in food and environmental analysis. However, several challenges are still present and thereby promising perspectives can be explored.

(1) To improve visualization, the process of building the sensor including the selection of fluorescent sources, the preparation of MIPs, and other aspects need to be optimized. Synthesizing new monomers or using multifunctional monomer imprinting strategies to improve selectivity, increasing the use of fluorescence sources such as UCNPs, preparing MIPs by considering dummy template imprinting strategies to improve the stability of results, and trying multi-template imprinting strategies for multi-target sensitive analysis can be attempted. By directly synthesizing composite fluorescent nanoparticles, multi-step synthesis and cumbersome chemical modifications can be avoided, and the stability can be improved.

(2) At present, researchers have developed a variety of fluorescence sources, and the preparation methods of MIPs have

been relatively mature. These are described in detail in section 2. However, there is still little attention to the questions of “what kind of luminescent materials are suitable for molecular imprinting, or what needs to improve luminescence performance” and “what preparation methods are required for molecularly imprinted fluorescent sensors, or what performance-oriented requirements are needed in the preparation method”. For example, theoretically, all light-emitting materials can actually be used to construct MI-RFL sensors. However, in practical applications, it is found that luminescent materials with the following properties are more suitable as fluorescence sources for MI-RFL sensors: (i) high fluorescence intensity and good fluorescence stability, such as QDs and CDs, which are difficult to be affected by acid–base solutions or other synthetic reagents; (ii) have functional groups that can bind to imprinted molecules, which is convenient for modification, such as the carboxyl group commonly used to modify QDs; and (iii) fluorescent materials that are specific for specific analytes also contribute to the subsequent provision of good selectivity. What's more, MIT should be fully combined with other techniques to prepare high-selectivity MIPs and thereby improve the analytical performances of MI-RFL sensors, such as orientation technology, aptamer technology, and boron affinity technology.

(3) In the field of environmental analysis, screening and identification of new pollutants including volatile organic compounds (VOCs) and microplastics are less performed. MI-RFL sensor applications for the analysis of VOC and microplastics, and various matrices such as gases, soil and sediments have promising prospects.

(4) In the field of food analysis, due to the characteristics of samples that are not easy to store or transport, the research direction of MI-RFL sensors will aim at micro-devices suitable for on-site and rapid detection. For ensuring food safety, not only is it necessary to detect the substances in it, but also to increase the detection in the whole chain of processing and transportation, so as to better ensure “safety at the tip of the tongue”.

(5) With the rapid development and wide application of MI-RFL sensors, they will face the challenge of complying with the requirements of green and sustainable development, and at present, there are still few studies on green imprinting.<sup>106,118</sup> There is a lot of room for the development of environmentally friendly MI-RFL sensors.

(6) At present, there are many studies on dual-emission MI-RFL sensors, while there are few related studies on ternary-emission MI-RFL sensors, which need to be vigorously carried out. PIMix and PIMod are ideal construction strategies. In addition, MI-RFL sensors are still in the proof-of-concept stage, and research on related portable devices should be increased in the future, and MI-RFL sensors should be commercialized. Especially, the ternary-emission MI-RFL sensors still face other challenges, for example as follows. (i) The visualization effects are expected to be further strengthened. Both reasonable modulation of fluorescent colors and extending the color change window are key measures. (ii) The detection sen-

sitivity is not high enough, and how to utilize the recognition ability of MIPs to modulate the interaction between fluorophores to achieve ultrasensitive detection is an important consideration. (iii) The applicability of such sensors in complicated matrices has always been the bottleneck of challenges and is a future research effort direction. So, the application of new sensors in environmental/food analysis should also be continuously explored. (iv) Related detection studies about gases by such sensors are still absent. Several issues are required to be addressed, such as the lack of a standardized composition scheme, inhomogeneity of binding sites, gas molecule recognition, and improper adhesion to the sensor surface. Furthermore, the trend towards gas sensors is miniaturization and sensor arrays.

MI-RFL sensors have been a hot topic in recent years, and the research on their design and application needs to be further explored. With the continuous maturity of green imprinting technology and the continuous optimization of sensor-based microdevices, MI-RFL sensors will develop towards more economical, efficient, environmentally friendly and portable directions. And the applications of MI-RFL sensors will be greatly expanded from environmental and food analysis to even other fields.

## Author contributions

Yuhao Wen: investigation and writing original draft. Dani Sun: review and editing. Yue Zhang: investigation and resources. Zhong Zhang: review and editing. Lingxin Chen: review and editing. Jinhua Li: conceptualization, supervision, and review and editing.

## Conflicts of interest

There are no conflicts to declare.

## Acknowledgements

This work was funded by the National Natural Science Foundation of China (No. 22176210, 21976209), Natural Science Foundation of Shandong Province (No. ZR2020KC032), Yantai Science and Technology Innovation Development Program (No. 2020MSGY077), Shaanxi Normal University Climbing Scholar Program (No. GK202206038) and Taishan Scholar Distinguished Expert Program (No. TS20190962).

## References

- 1 Y. Han, W. Yang, X. Luo, X. He, H. Zhao, W. Tang, T. Yue and Z. Li, *Crit. Rev. Food Sci. Nutr.*, 2022, **62**, 244–260.
- 2 S. Farooq, H. Wu, J. Nie, S. Ahmad, I. Muhammad, M. Zeeshan, R. Khan and M. Asim, *Sci. Total Environ.*, 2022, **804**, 150293.

- 3 Z. Sun, Y. Lu, L. Zhu, W. Liu, Y. Qu, N. Lin and P. Yu, *J. Chem. Technol. Biotechnol.*, 2019, **94**, 2917–2927.
- 4 S. Bajkacz, E. Felis, E. Kycia-Slocka, M. Harnisz and E. Korzeniewska, *Sci. Total Environ.*, 2020, **726**, 138071.
- 5 Y. Feng, W. J. Zhang, Y. W. Liu, J. M. Xue, S. Q. Zhang and Z. J. Li, *Molecules*, 2018, **23**, 1953.
- 6 D. J. Denmark, S. Mohapatra and S. S. Mohapatra, *EuroBiotech J.*, 2020, **4**, 184–206.
- 7 M. Jia, Z. Zhang, J. Li, X. Ma, L. Chen and X. Yang, *TrAC, Trends Anal. Chem.*, 2018, **106**, 190–201.
- 8 R. Park, S. Jeon, J. Jeong, S. Y. Park, D. W. Han and S. W. Hong, *Biosensors*, 2022, **12**, 136.
- 9 H. Yang, H. Liu, Z. Tang, Z. Qiu, H. Zhu, Z. Song and A. Jia, *J. Environ. Chem. Eng.*, 2021, **9**, 106352.
- 10 L. Chen, X. Wang, W. Lu, X. Wu and J. Li, *Chem. Soc. Rev.*, 2016, **45**, 2137–2211.
- 11 X. Yang, Z. Zhang, J. Li, M. Jia and L. Chen, *Sci. Sin.: Chim.*, 2017, **47**, 300–314.
- 12 Y. Wen, D. Sun, Y. Zhang, N. Zhou, H. Liu, J. Li and X. Zhuang, *Chem. Reagents*, 2022, **44**, 1334–1341.
- 13 H. Jin, M. Yang, Z. Sun and R. Gui, *Coord. Chem. Rev.*, 2021, **446**, 214114.
- 14 D. Wang, X. Fan, S. Sun, S. Du, H. Li, J. Zhu, Y. Tang, M. Chang and Y. Xu, *Sens. Actuators, B*, 2018, **264**, 304–311.
- 15 Q. Yang, C. Li, J. Li, M. Arabi, X. Wang, H. Peng, H. Xiong, J. Choo and L. Chen, *J. Mater. Chem. C*, 2020, **8**, 5554–5561.
- 16 J. Li and D. Sun, *Langmuir*, 2022, **38**, 13305–13312.
- 17 J. J. Li, D. Qiao, J. Zhao, G. J. Weng, J. Zhu and J. W. Zhao, *Methods Appl. Fluoresc.*, 2019, **7**, 045001.
- 18 X. Hu, Y. Guo, T. Wang, C. Liu, Y. Yang and G. Fang, *J. Hazard. Mater.*, 2022, **421**, 126748.
- 19 J. Fu, S. Zhou, X. Wu, S. Tang, P. Zhao, K. Tang, Y. Chen, Z. Yang, Z. Zhang and H. Chen, *Environ. Pollut.*, 2022, **309**, 119762.
- 20 D. C. Apodaca, R. B. Pernites, R. R. Ponnappati, F. R. Del Mundo and R. C. Advincula, *ACS Appl. Mater. Interfaces*, 2011, **3**, 191–203.
- 21 M. Hussain, N. Iqbal and P. A. Lieberzeit, *Sens. Actuators, B*, 2013, **176**, 1090–1095.
- 22 N. Karimian, M. H. A. Zavar, M. Chamsaz, A. P. F. Turner and A. Tiwari, *Electrochem. Commun.*, 2013, **36**, 92–95.
- 23 J. Li, X. Huang, J. Ma, S. Wei and H. Zhang, *Ionics*, 2020, **26**, 4183–4192.
- 24 M. V. Sullivan, A. Henderson, R. A. Hand and N. W. Turner, *Anal. Bioanal. Chem.*, 2022, **414**, 3687–3696.
- 25 Q. Luo, N. Yu, C. Shi, X. Wang and J. Wu, *Talanta*, 2016, **161**, 797–803.
- 26 D. Sun, Z. Song, Y. Zhang, Y. Wang, M. Lv, H. Liu, L. Wang, W. Lu, J. Li and L. Chen, *Front. Environ. Chem.*, 2021, **2**, 703961.
- 27 M. Arabi, A. Ostovan, A. R. Bagheri, X. Guo, L. Wang, J. Li, X. Wang, B. Li and L. Chen, *TrAC, Trends Anal. Chem.*, 2020, **128**, 115923.
- 28 M. Haroon, M. Tahir, H. Nawaz, M. I. Majeed and A. A. Al-Saadi, *Photodiagn. Photodyn. Ther.*, 2022, **37**, 102690.
- 29 Y. Lu, Q. Liu, B. Fu, P. Li and W. Xu, *Talanta*, 2023, **258**, 124461.
- 30 L. Wang, X. Wang, L. Cheng, S. Ding, G. Wang, J. Choo and L. Chen, *Biosens. Bioelectron.*, 2021, **189**, 113360.
- 31 M. Arabi, A. Ostovan, Y. Wang, R. Mei, L. Fu, J. Li, X. Wang and L. Chen, *Nat. Commun.*, 2022, **13**, 5757.
- 32 Q. Yang, J. Li, X. Wang, H. Peng, H. Xiong and L. Chen, *Biosens. Bioelectron.*, 2018, **112**, 54–71.
- 33 F. Yang, Q. Zhang, S. Huang and D. Ma, *J. Mater. Chem. B*, 2020, **8**, 7856–7879.
- 34 Y. Chen, X. Wang, C. Lu, W. Wu and X. Wang, *Food Control*, 2021, **129**, 108218.
- 35 X. Zhao, C. Lei, Y. Gao, H. Gao, S. Zhu, X. Yang, J. You and H. Wang, *Sens. Actuators, B*, 2017, **253**, 239–246.
- 36 S. H. Park, N. Kwon, J. H. Lee, J. Yoon and I. Shin, *Chem. Soc. Rev.*, 2020, **49**, 143–179.
- 37 W. Pei, L. Han, Y. Su and G. Li, *New Chem. Mater.*, 2020, **48**, 1–5.
- 38 T. S. Ponomaryova, A. S. Novikova, A. M. Abramova, O. A. Goryacheva, D. D. Drozd, P. D. Strokin and I. Y. Goryacheva, *J. Anal. Chem.*, 2022, **77**, 402–409.
- 39 J. Xiong, H. Zhang, L. Qin, S. Zhang, J. Cao and H. Jiang, *Int. J. Mol. Sci.*, 2022, **23**, 4088.
- 40 Y. Wen, D. Sun, J. Yu, J. Qi, Z. Zhang, Z. Song, X. Wang, H. Liu, L. Chen and J. Li, *Sci. Sin.: Chim.*, 2023, **53**, 196–206.
- 41 J. Wu, W. Xin, Y. Wu, Y. Zhan, J. Li, J. Wang, S. Huang and X. Wang, *Chem. Eng. J.*, 2021, **422**, 130158.
- 42 Z. Fatahi, N. Esfandiari and Z. Ranjbar, *J. Anal. Test.*, 2020, **4**, 307–315.
- 43 Y. Hu, Z. Yang, X. Lu, J. Guo, R. Cheng, L. Zhu, C. F. Wang and S. Chen, *Nanoscale*, 2020, **12**, 5494–5500.
- 44 P. Yu, X. Wen, Y.-R. Toh, X. Ma and J. Tang, *Part. Part. Syst. Charact.*, 2015, **32**, 142–163.
- 45 Y. Xia, K. Sun, Y.-N. Zuo, S. Zhu and X. Zhao, *Chin. Chem. Lett.*, 2022, **33**, 2081–2085.
- 46 X. Wang, L. Li, L. Li, T. Bu, K. Yang, J. Xia, X. Sun, H. Jiang and L. Wang, *Mikrochim. Acta*, 2022, **189**, 402.
- 47 Q. Yang, C. Li, J. Li, X. Wang, M. Arabi, H. Peng, H. Xiong and L. Chen, *Nanoscale*, 2020, **12**, 6529–6536.
- 48 M. Chen, Z. Liang, G. Zeng, Y. Wang, Z. Mai, X. Chen, G. Wu and T. Chen, *Dyes Pigm.*, 2022, **198**, 109995.
- 49 H. Jin, Z. Sun, Y. Sun and R. Gui, *TrAC, Trends Anal. Chem.*, 2021, **134**, 116124.
- 50 X. Wang, J. Yu, Q. Kang, D. Shen, J. Li and L. Chen, *Biosens. Bioelectron.*, 2016, **77**, 624–630.
- 51 T. Arslan and O. Guney, *Anal. Biochem.*, 2020, **591**, 113540.
- 52 N. S. Amiri and M.-R. Milani-Hosseini, *Anal. Methods*, 2019, **11**, 5919–5928.
- 53 M. Rong, D. Wang, Y. Li, Y. Zhang, H. Huang, R. Liu and X. Deng, *J. Anal. Test.*, 2021, **5**, 51–59.
- 54 M. Liu, Z. Gao, Y. Yu, R. Su, R. Huang, W. Qi and Z. He, *Nanoscale Res. Lett.*, 2018, **13**, 27.

- 55 Y. Fu, H. Jin, X. Bu and R. Gui, *J. Mater. Chem. C*, 2019, **7**, 11483–11492.
- 56 A. I. Ayesh, *J. Nanomater.*, 2016, **2016**, 1–17.
- 57 H. Lu and S. Xu, *Biosens. Bioelectron.*, 2017, **92**, 147–153.
- 58 C. Li, Q. Yang, X. Wang, M. Arabi, H. Peng, J. Li, H. Xiong and L. Chen, *Food Chem.*, 2020, **319**, 126575.
- 59 C. Gong, Z. Li, G. Liu, R. Wang and S. Pu, *Spectrochim. Acta, Part A*, 2022, **265**, 120362.
- 60 Q. Yang, J. Li, X. Wang, H. Peng, H. Xiong and L. Chen, *Sens. Actuators, B*, 2019, **284**, 428–436.
- 61 S. Kamal, M. Khalid, M. S. Khan and M. Shahid, *Coord. Chem. Rev.*, 2023, **474**, 214859.
- 62 X. Wang, J. Yu, X. Wu, J. Fu, Q. Kang, D. Shen, J. Li and L. Chen, *Biosens. Bioelectron.*, 2016, **81**, 438–444.
- 63 Y. Chen, J. W. Y. Lam, R. T. K. Kwok, B. Liu and B. Z. Tang, *Mater. Horiz.*, 2019, **6**, 428–433.
- 64 A. Rico-Yuste and S. Carrasco, *Polymers*, 2019, **11**, 1173.
- 65 L. Wang, J. Yang, L. Tang, L. Luo, C. Chen, H. Gong and C. Cai, *Mikrochim. Acta*, 2021, **188**, 221.
- 66 X. Wang, J. Li and L. Chen, *Chin. Sci. Bull.*, 2019, **64**, 1352–1367.
- 67 Y. Zhang, G. Zhao, K. Han, D. Sun, N. Zhou, Z. Song, H. Liu, J. Li and G. Li, *Molecules*, 2023, **28**, 301.
- 68 Y. Jin, *J. New Ind.*, 2022, **12**, 59–63.
- 69 Q. Li, W. Zhang, X. Liu and H. Zhang, *Mikrochim. Acta*, 2022, **189**, 464.
- 70 Z. Jiang, Q. Li, Q. Li, H. Xu, J. He, C. Wang, L. Zhou, Q. Zhang, L. Luo and C. Yuan, *Microchem. J.*, 2022, **179**, 107545.
- 71 Z. Qi, C. Xiang, X. Tian and X. Xu, *Foods*, 2022, **11**, 3239.
- 72 J. Li, Y. Wang and X. Yu, *Front. Chem.*, 2021, **9**, 706311.
- 73 J. Li, J. Fu, Q. Yang, L. Wang, X. Wang and L. Chen, *Analyst*, 2018, **143**, 3570–3578.
- 74 L. Wang, J. Li, J. Wang, X. Guo, X. Wang, J. Choo and L. Chen, *J. Colloid Interface Sci.*, 2019, **541**, 376–386.
- 75 W. Liu, X. Wang, Y. Wang, J. Li, D. Shen, Q. Kang and L. Chen, *Sens. Actuators, B*, 2018, **262**, 810–817.
- 76 H. Lu, D. Wei, R. Zheng and S. Xu, *Analyst*, 2019, **144**, 6283–6290.
- 77 H. Zhu, T. Yu, H. Xu, K. Zhang, H. Jiang, Z. Zhang, Z. Wang and S. Wang, *ACS Appl. Mater. Interfaces*, 2014, **6**, 21461–21467.
- 78 W. Li, H. Zhang, S. Chen, Y. Liu, J. Zhuang and B. Lei, *Biosens. Bioelectron.*, 2016, **86**, 706–713.
- 79 Q. Yang, J. Li, X. Wang, H. Xiong and L. Chen, *Anal. Chem.*, 2019, **91**, 6561–6568.
- 80 X. Hu, Y. Guo, J. Zhang, X. Wang, G. Fang and S. Wang, *Chem. Eng. J.*, 2022, **433**, 134499.
- 81 X. Wu, S. Tang, P. Zhao, K. Tang, Y. Chen, J. Fu, S. Zhou, Z. Yang and Z. Zhang, *Food Chem.*, 2023, **402**, 134256.
- 82 X. Zhu, L. Han, H. Liu and B. Sun, *Food Chem.*, 2022, **379**, 132154.
- 83 X. Liu, T. Wang and Y. Wang, *Anal. Chim. Acta*, 2023, **1240**, 340728.
- 84 M. Yang, C. Wang, E. Liu, X. Hu, H. Hao and J. Fan, *J. Mol. Liq.*, 2021, **337**, 116438.
- 85 X. Wang, S. Yu, J. Wang, J. Yu, M. Arabi, L. Fu, B. Li, J. Li and L. Chen, *Talanta*, 2020, **211**, 120727.
- 86 S. Xu, Y. Zou and H. Zhang, *Talanta*, 2020, **211**, 120711.
- 87 J. Wang, X. Chen, X. Wang, Q. Kang, D. Shen and L. Chen, *Sens. Actuators, B*, 2020, **322**, 128581.
- 88 Y. Hou, Y. Zou, Y. Zhou and H. Zhang, *Langmuir*, 2020, **36**, 12403–12413.
- 89 H. Ran, Z. Lin, C. Hong, J. Zeng, Q. Yao and Z.-Y. Huang, *J. Photochem. Photobiol., A*, 2019, **372**, 260–269.
- 90 Y. Li, W. He, Q. Peng, L. Hou, J. He and K. Li, *Food Chem.*, 2019, **287**, 55–60.
- 91 X. Wei and H. Chen, *Anal. Bioanal. Chem.*, 2019, **411**, 5809–5816.
- 92 X. Chen, Y. Luan, N. Wang, Z. Zhou, X. Ni, Y. Cao, G. Zhang, Y. Lai and W. Yang, *J. Sep. Sci.*, 2018, **41**, 4394–4401.
- 93 L. Zhang and L. Chen, *Mikrochim. Acta*, 2018, **185**, 135.
- 94 L. Wang, L. Wen, S. Zheng, F. Tao, J. Chao, F. Wang and C. Li, *Sens. Actuators, B*, 2022, **361**, 131688.
- 95 P. Li, H. Fu, Z. Bai, X. Feng, J. Qi, X. Song, X. Hu and L. Chen, *Analyst*, 2023, **148**, 573–582.
- 96 J. Luo, H. Tan, B. Yang, D. Chen and J. Fei, *Anal. Methods*, 2022, **14**, 3881–3889.
- 97 T. Wu, B. Hu, J. Lv, Y. Li, J. Shao, Y. Ma and Y. Cui, *Opt. Mater.*, 2022, **132**, 112784.
- 98 J. J. You, H. Liu, R. R. Zhang, Q. F. Pan, A. L. Sun, Z. M. Zhang and X. Z. Shi, *Sci. Total Environ.*, 2022, **848**, 157675.
- 99 Y. Xu, T. Huang, B. Hu, M. Meng and Y. Yan, *Microchem. J.*, 2022, **172**, 106899.
- 100 Y. Ma, X. Jin, Y. Xing, G. Ni and J. Peng, *Anal. Methods*, 2019, **11**, 2033–2040.
- 101 X. Wang, J. Yu, J. Li, Q. Kang, D. Shen and L. Chen, *Sens. Actuators, B*, 2018, **255**, 268–274.
- 102 W. Gui, H. Wang, Y. Liu and Q. Ma, *Sens. Actuators, B*, 2018, **266**, 685–691.
- 103 M. Li, H. Liu and X. Ren, *Biosens. Bioelectron.*, 2017, **89**, 899–905.
- 104 R. Jalili and A. Khataee, *Food Chem. Toxicol.*, 2020, **146**, 111806.
- 105 Q. Shi, J. Fu, J. Chen and Y. Zhou, *Chem. Reagents*, 2022, **44**, 1342–1349.
- 106 D. J. C. Constable, *iScience*, 2021, **24**, 103489.
- 107 B. S. Rathi, P. S. Kumar and P. L. Show, *J. Hazard. Mater.*, 2021, **409**, 124413.
- 108 V. Padmanabhan, W. Song and M. Puttabyatappa, *Endocr. Rev.*, 2021, **42**, 295–353.
- 109 G. Zhao, Y. Zhang, D. Sun, S. Yan, Y. Wen, Y. Wang, G. Li, H. Liu, J. Li and Z. Song, *Molecules*, 2023, **28**, 335.
- 110 F. Liu, Y. Zhang, J. Qi, B. Li, X. Han, Y. Shi, Z. Song, J. Han and H. Xu, *Sci. Sin.: Chim.*, 2020, **50**, 463–475.
- 111 N. Z. Arman, S. Salmiati, A. Aris, M. R. Salim, T. H. Nazifa, M. S. Muhamad and M. Marpongahtun, *Water*, 2021, **13**, 3258.
- 112 M. S. Sharifzadeh, G. Abdollahzadeh, C. A. Damalas, R. Rezaei and M. Ahmadyousefi, *Sci. Total Environ.*, 2019, **651**, 2953–2960.

- 113 O. Jamieson, F. Mecozzi, R. D. Crapnell, W. Battell, A. Hudson, K. Novakovic, A. Sachdeva, F. Canfarotta, C. Herdes, C. E. Banks, H. Snyder and M. Peeters, *Phys. Status Solidi A*, 2021, **218**, 2100021.
- 114 Y. Ye, T. Wu, X. Jiang, J. Cao, X. Ling, Q. Mei, H. Chen, D. Han, J. J. Xu and Y. Shen, *ACS Appl. Mater. Interfaces*, 2020, **12**, 14552–14562.
- 115 Y. Zhan, Y. Zeng, L. Li, F. Luo, B. Qiu, Z. Lin and L. Guo, *ACS Sens.*, 2019, **4**, 1252–1260.
- 116 J. Xu, *China Food Safety Magazine*, 2022, vol. 08, pp. 34–36.
- 117 G. Hao, L. Chen, Z. Zhang, X. Ma, J. Li and X. Yang, *Sci. Sin.: Chim.*, 2020, **50**, 393–405.
- 118 M. Arabi, A. Ostovan, J. Li, X. Wang, Z. Zhang, J. Choo and L. Chen, *Adv. Mater.*, 2021, **33**, 2100543.